Monthly Notices
of the
ROYAL ASTRONOMICAL SOCIETY

Mon. Not. R. Astron. Soc. **410,** 27–32 (2011) doi:10.1111/j.1365-2966.2010.17419.x

Probing the nature of high-z short GRB 090426 with its early optical and X-ray afterglows

Li-Ping Xin,[1⋆] En-Wei Liang,[2⋆] Jian-Yan Wei,[1] Bing Zhang,[3] Hou-Jun Lv,[2] Wei-Kang Zheng,[4] Yuji Urata,[5] Myungshin Im,[6] Jing Wang,[1] Yu-Lei Qiu,[1] Jin-Song Deng,[1] Kui-Yun Huang,[5] Jing-Yao Hu,[1] Yiseul Jeon,[6] Hua-Li Li[1] and Xu-Hui Han[1]

[1]*National Astronomical Observatories, Chinese Academy of Sciences, Beijing 100012, China*
[2]*Department of Physics, Guangxi University, Guangxi 530004, China*
[3]*Department of Physics and Astronomy, University of Nevada, Las Vegas, Nv 89154, USA*
[4]*Department of Physics, University of Michigan, Ann Arbor, MI 48109, USA*
[5]*Institute of Astronomy and Astrophysics, Academia Sinica, PO Box 23-141, Taipei 106, Taiwan*
[6]*Centre for the Exploration of the Origin of the Universe, Department of Physics & Astronomy, FPRD, Seoul National University, Shillim-dong, San 56-1, Kwanak-gu, Seoul, Korea*

Accepted 2010 July 24. Received 2010 June 21; in original form 2010 February 3

ABSTRACT

GRB 090426 is a short-duration burst detected by *Swift* ($T_{90} \sim 1.28$ s in the observer frame and $T_{90} \sim 0.33$ s in the burst frame at $z = 2.609$). Its host galaxy properties and some gamma-ray-related correlations are analogous to those seen in long-duration gamma-ray bursts (GRBs), which are believed to be of a massive star origin (so-called Type II GRBs). We present the results of its early optical observations with the 0.8-m Tsinghua University–National Astronomical Observatory of China Telescope (TNT) at Xinglong Observatory and the 1-m LOAO telescope at Mt Lemmon Optical Astronomy Observatory in Arizona. Our well-sampled optical afterglow light curve covers from ∼90 to 10^4 s after the GRB trigger. It shows two shallow decay episodes that are likely due to energy injection, which end at ∼230 and 7100 s, respectively. The decay slopes after the injection phases are consistent with each other ($\alpha \simeq 1.22$). The X-ray afterglow light curve appears to trace the optical, although the second energy-injection phase was missed due to visibility constraints introduced by the *Swift* orbit. The X-ray spectral index is $\beta_X \sim 1.0$ without temporal evolution. Its decay slope is consistent with the prediction of the forward shock model. Both X-ray and optical emission are consistent with being in the same spectral regime above the cooling frequency (ν_c). The fact that ν_c is below the optical band from the very early epoch of the observation provides a constraint on the burst environment, which is similar to that seen in classical long-duration GRBs. We therefore suggest that death of a massive star is the possible progenitor of this short burst.

Key words: gamma-ray burst: individual: GRB 090426 – gamma-rays: general.

1 INTRODUCTION

Cosmic gamma-ray bursts (GRBs) are classified into two classes with a separation at the observed burst duration of $T_{90} \sim 2$ s based on *CGRO*/BATSE observations (Kouveliotou et al. 1993). The afterglow and host galaxy properties of long GRBs, especially the detections of several long GRB–supernova associations (e.g. Galama et al. 1998; Hjorth et al. 2003; Soderberg et al. 2004; Campana et al. 2006), suggest that they are most likely related to deaths of massive stars. The 'collapsar' model has been widely recognized as the standard scenario for long GRBs (Woosley 1993; Paczyński 1998; Piran 2004; Zhang & Mészáros 2004; Woosley & Bloom 2006). In the *Swift* era, the afterglows and host galaxies of some short GRBs have been identified (Berger et al. 2005; Fox et al. 2005; Gehrels et al. 2005; Villasenor et al. 2005; McGlynn et al. 2008). Some short GRBs are found to be associated with nearby early-type galaxies with little star formation. Some others are

⋆E-mail: xlp@bao.ac.cn (L-PX); lew@gxu.edu.cn (E-WL)

located in late-type star-forming galaxies (e.g. Fox et al. 2005; Fong, Berger & Fox 2010), some of which are at high redshifts (Levan et al. 2006; Berger et al. 2007). No short-duration GRB was found to be associated with a supernova (Kann et al. 2008; Zhang et al. 2009, and references therein). All these seem to favour the idea that short GRBs are from mergers of two compact stellar objects (Eichler et al. 1989; Narayan, Paczyński & Piran 1992).

Later *Swift* observations have revealed that the short/long separation is not sufficiently clean to differentiate their physical origins. This led to the introduction of the physical classification scheme Type II (collapses of massive stars) versus Type I (putatively identified as mergers) GRBs (Kann et al. 2007, 2008; Zhang et al. 2007a, 2009; Lv et al. 2010). Some convincing Type I GRBs have long, soft 'extended emission' (Barthelmy et al. 2005; Norris & Bonnell 2006; Lin et al. 2008; Perley et al. 2009; Zhang et al. 2009), making their T_{90} 'long'. The non-detection of any supernovae associated with the nearby long GRBs 060614 and 060505 (Fynbo et al. 2006; Gal-Yam et al. 2006; Gehrels et al. 2006) casted doubts on the Type II origin for these long GRBs. Some long GRBs have rest-frame durations shorter than 2 s (Levan et al. 2007). Observations of two intrinsically short-duration, high-z GRBs 080913 ($z = 6.7$; Greiner et al. 2009) and 090423 ($z = 8.3$; Salvaterra et al. 2009; Tanvir et al. 2009) suggest that they share a lot of common properties with long GRBs, and most likely have a massive star progenitor (Lin et al. 2010; Zhang et al. 2009; Belczynski et al. 2010; Levesque et al. 2010a). Virgili et al. (2009) and Zhang et al. (2009) suggested that some (or even most) short-duration GRBs are probably not produced via compact star mergers (Type I), but are likely related to massive stars (Type II). Based on the observed gamma-ray energy and peak energy of the νf_ν spectrum of prompt gamma-ray emission, Lv et al. (2010) defined a parameter $\varepsilon \equiv E_{\rm iso}/E_{\rm p,z}^{1.7}$, and proposed a new empirical classification scheme that is found to better match the physically motivated Type II/I classification scheme. They showed that the typical Type II GRBs are in the high-ε group, in contrast to the typical Type I GRBs that belong to the low-ε group.

Another striking case that poses a challenge to the conventional long versus short GRB classification scheme is GRB 090426. This burst has an observed $T_{90} = 1.29 \pm 0.09$ s in the *Swift* Burst Alert Telescope (BAT) band (Sato et al. 2009), corresponding to a burst rest-frame duration of 0.33 s at redshift $z = 2.609$ (Levesque et al. 2010a). Phenomenologically, in terms of duration alone, it is unambiguously within the range of classical short-type GRBs in both the observer frame and the burst rest frame. On the other hand, both the host galaxy properties (Levesque et al. 2010a) and the spectral energy properties (Antonelli et al. 2009) suggest that it is most likely a Type II GRB, i.e. related to core collapse of a massive star. With the new classification method proposed by Lv et al. (2010), this event is also well classified into the high-ε group, which is where all known Type II GRBs belong to.

Multiwavelength afterglows are essential for revealing the burst environment, and hence can serve as a probe of the GRB progenitor. In this paper, we report our observations of the early optical afterglow for GRB 090426 using the Tsinghua University–National Astronomical Observatory of China Telescope (TNT) at Xinglong Observatory and the LOAO telescope at Mt Lemmon Optical Astronomy Observatory in Arizona. We use the optical and X-ray afterglow data to explore the nature of this event. Our observations are reported in Section 2. A joint optical and X-ray data analysis is presented in Section 3. Conclusions and discussion are presented in Section 4. The notation $f_\nu \propto t^{-\alpha}\nu^{-\beta}$ is used throughout the paper, where f_ν is the spectral flux density at the frequency ν.

2 OBSERVATIONS

GRB 090416 was detected by *Swift* BAT at 12:48:47 UT on 2009 April 26 (Cummings et al. 2009). Its duration is $T_{90} = 1.28 \pm 0.09$ s in 15–350 keV. The *Swift* X-ray Telescope (XRT) began to observe the burst since 84.6 s after the GRB trigger. At 89 s after the trigger, the *Swift* UVOT began to observe the burst and reported an optical counterpart with a brightness of about 17.5 mag in the white band. The optical afterglow was confirmed by the Xinglong TNT (Xin et al. 2009) and other follow-up observations (e.g. Im et al. 2009). A redshift of 2.609 was determined by Levesque et al. (2009) using the Keck telescope, which was confirmed by the European Southern Observatory (ESO) Very Large Telescope (VLT) observation (Thoene et al. 2009). The time-integrated gamma-ray spectrum is well fitted by a power law with a photon index Γ of 1.93 (Sato et al. 2009; $\beta = \Gamma - 1$), which roughly corresponds to an estimated spectral peak energy (in the observer frame) $E_{\rm p,obs} \sim 45$ keV using an empirical relation between $E_{\rm p}$ and the power-law photon index of the BAT spectrum (Zhang et al. 2007a; Sakamoto et al. 2009).

2.1 Optical observation and data reduction

We carried out a follow-up observation campaign of GRB 090426 using the 0.8-m TNT at Xinglong Observatory, under the framework of East-Asia GRB Follow-up Observation Network (EAFON; Urata et al. 2003, 2005). TNT is equipped with a PI 1300 × 1340 CCD and filters in the standard Johnson–Bessel system. Its field of view is 11.4 × 11.4 arcmin^2, yielding a 0.5-arcsec pixel scale. A custom-designed automation system has been developed for the GRB follow-up observations (Zheng et al. 2008).

The observation of the optical transient (OT) of GRB 090426 was carried out with TNT at 86 s after the *Swift*/BAT trigger, which is slightly earlier than the beginning observation of XRT and UVOT on board *Swift*. A new fading source was discovered and confirmed as the OT of the burst (Xin et al. 2009). The coordinates of the OT are consistent with that of UVOT (Cummings et al. 2009). The *W*-(white), *R*- and *V*-band images were obtained in 86–519, 570–1513 and 1907–10 748 s after the GRB trigger, respectively.

The 1-m telescope (Han et al. 2005; Lee, Im & Urata 2010) is located at Mt Lemmon Optical Astronomy Observatory (LOAO) in Arizona operated by the Korea Astronomy and Space Science Institute. The observation of GRB 090426 was carried out at about 16.3 h after the burst ($t \sim 60$ ks) in the *R* filter. The OT was not detected and only upper limits were obtained.

Data reduction was carried out following the standard routine in IRAF[1] package, including bias and flat-field corrections. Dark correction was not performed since the temperature of our CCD was cooled down to -110°C. Point spread function (PSF) photometry was applied via the DAOPHOT task in the IRAF package to obtain the instrumental magnitudes. During the reduction, some frames were combined in order to increase the signal-to-noise ratio (S/N). In the calibration and analysis, the white band was treated as the *R* band (Xin et al. 2010). Absolute calibration was performed using the Sloan Digital Sky Survey (SDSS; Adelman-McCarthy et al. 2008), with conversion of SDSS to Johnson–Cousins system.[2] The data of GRB 090426 obtained by TNT and LOAO are reported in Table 1.

[1] IRAF is distributed by National Optical Astronomy Observatories (NOAO), which is operated by AURA, Inc., under cooperative agreement with NSF.
[2] http://www.sdss.org/dr6/algorithms/sdssUBVRITransform.html #Lupton2005

Table 1. Optical afterglow photometry log of GRB 090426. The reference time T_0 is *Swift* BAT burst trigger time. All data are not corrected for the Galactic extinction [which is $E(B-V)=0.017$; Schlegel et al.1998]. 'Merr' means the uncertainty of magnitude.

$T-T_0$ (mid) (s)	Exposure (s)	Mag	Merr	Filter	Telescope
86	20.0	16.44	0.03	*W*	TNT
109	20.0	16.50	0.03	*W*	TNT
133	20.0	16.59	0.03	*W*	TNT
155	20.0	16.66	0.03	*W*	TNT
178	20.0	16.76	0.03	*W*	TNT
201	20.0	16.88	0.04	*W*	TNT
223	20.0	17.01	0.04	*W*	TNT
246	20.0	17.01	0.04	*W*	TNT
269	20.0	17.07	0.04	*W*	TNT
292	20.0	17.09	0.04	*W*	TNT
314	20.0	17.22	0.04	*W*	TNT
337	20.0	17.30	0.05	*W*	TNT
360	20.0	17.31	0.05	*W*	TNT
382	20.0	17.44	0.05	*W*	TNT
405	20.0	17.50	0.06	*W*	TNT
428	20.0	17.56	0.06	*W*	TNT
451	20.0	17.69	0.06	*W*	TNT
473	20.0	17.63	0.06	*W*	TNT
496	20.0	17.80	0.06	*W*	TNT
519	20.0	17.89	0.06	*W*	TNT
570	60.0	17.93	0.06	*R*	TNT
649	60.0	18.12	0.07	*R*	TNT
728	60.0	18.30	0.07	*R*	TNT
807	60.0	18.38	0.08	*R*	TNT
885	60.0	18.46	0.09	*R*	TNT
964	60.0	18.72	0.08	*R*	TNT
1042	60.0	18.71	0.08	*R*	TNT
1121	60.0	18.78	0.11	*R*	TNT
1199	60.0	18.85	0.11	*R*	TNT
1278	60.0	19.01	0.11	*R*	TNT
1356	60.0	19.04	0.12	*R*	TNT
1435	60.0	19.12	0.12	*R*	TNT
1513	60.0	19.06	0.12	*R*	TNT
1907	300 × 2	19.72	0.12	*V*	TNT
2542	300 × 2	20.04	0.12	*V*	TNT
3178	300 × 2	20.10	0.12	*V*	TNT
3813	300 × 2	20.05	0.12	*V*	TNT
4448	300 × 2	20.17	0.12	*V*	TNT
5084	300 × 2	20.19	0.14	*V*	TNT
5878	300 × 3	20.30	0.14	*V*	TNT
7048	600 × 2	20.47	0.16	*V*	TNT
8282	600 × 2	20.69	0.17	*V*	TNT
9515	600 × 2	20.65	0.17	*V*	TNT
10 748	600 × 2	20.71	0.18	*V*	TNT
58 591	180 × 10	>21.67		*R*	LOAO

2.2 *Swift*/XRT X-ray afterglow data reduction

The *Swift*/XRT light curve and spectrum are extracted from the UK *Swift* Science Data Centre at the University of Leicester (Evans et al. 2009).[3] We fit the X-ray spectrum with the XSPEC package. The time-integrated X-ray spectrum is well fitted by an absorbed power-law model, with a photon power-law index $\Gamma = 2.00 \pm 0.06$ from the PC mode data. No significant host N_H excess over the Galactic value is detected.

[3] http://www.swift.ac.uk/results.shtml

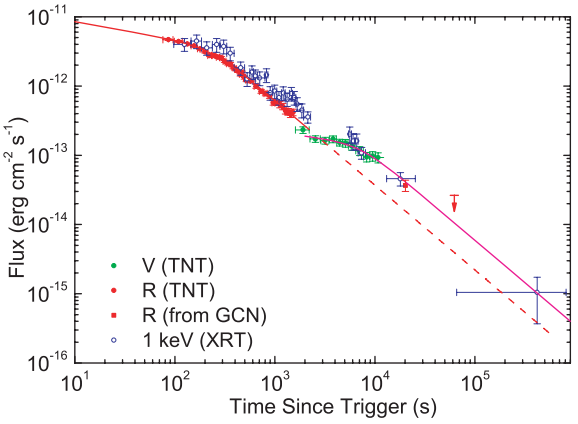

Figure 1. The extinction-corrected optical light curve of GRB 090426 (solid dots) and the best fit with a smooth broken power-law model (solid line) for two epochs 2200 s before and after the GRB trigger. The *R*-band data observed by Rumyantsev et al. (2009) is marked with squares. The XRT light curve (open dots) is also shown for comparison.

3 OPTICAL AND X-RAY AFTERGLOW JOINT ANALYSIS

3.1 Temporal analysis

With the X-ray spectral index ($\beta_X = 1.00 \pm 0.06$), we first derive the 1-keV light curve from the XRT data. It is shown in Fig. 1. Next, we convert the extinction-corrected magnitudes of the optical afterglow into energy fluxes. Levesque et al. (2010a) reported $A_V \sim 0.4$ for the GRB host galaxy, and the extinction by the Milky Way (MW) Galaxy in the burst direction is $E(B-V) = 0.017$ (Schlegel, Finkbeiner & Davis 1998). For the host galaxy, the transformation from A_V to A_R is nearly independent of any known type of extinction laws (MW, Large Magellanic Cloud, Small Magellanic Cloud), and we take $A_R \sim 0.32$ for the host galaxy. The MW extinction corresponds to $A_R = 0.046$ and $A_V = 0.057$. After extinction corrections, we find that the νF_ν fluxes in both the optical and the X-ray bands are almost the same. This indicates a flat νF_ν spectrum from the optical to the X-ray bands, i.e. $\beta_{OX} \sim 1.0$. This is consistent with the observed X-ray spectral index. This flat νF_ν spectrum also means that we do not need to calibrate the observed optical fluxes to a given band. The extinction-corrected optical energy flux light curve is also shown in Fig. 1.

As shown in Fig. 1, the afterglow light curves in the optical and X-ray bands trace with each other, suggesting that they not only are of similar (external shock) origin but also belong to the same spectral regime. At early epochs ($t < 2200$ s after the GRB trigger), the optical and X-ray afterglow light curves show a smooth shallow-to-normal transition in the decaying behaviour, with small flickerings in the X-ray band. In the time interval 2200–5500 s, the brightness of the OT was almost constant, fading again after $t > 5500$ s. The OT was also detected by Rumyantsev, Antoniuk & Pozanenko (2009) at 0.2342 d (20 200 s) after GRB trigger. It had faded to $R = 21.3 \pm 0.2$, indicating a decay slope of ~1.2 in the time interval of $t > 5500$ s. Due to the orbital constraints of the *Swift* satellite, there is no XRT observation in the time interval [2200, 5500] s when the optical light-curve features a plateau. The fading behaviour of X-rays in the time interval [5500, 7700] s is similar to that of the optical afterglow. At $t \sim 0.2342$ d, the detected X-ray behaviour is also consistent with that of the optical emission. These results suggest that the temporal behaviour of both optical

Table 2. Optical light-curve fits with a smooth broken power-law model for two epochs.

Interval (s)	F_0^a	t_p (s)	α_1	α_2
86–2200	3.74 ± 0.32	227 ± 27	0.26 ± 0.07	1.22 ± 0.04
>2200	1.77 ± 0.67	7123 ± 3620	0.19 ± 0.41	$\sim$1.22

[a]In units of $\times 10^{-12}$ erg cm^{-2} s^{-1}.

and X-ray afterglows could be the same. We thus perform a temporal analysis on the well-sampled optical light curve only. The optical light curves in the time intervals both before and after 2200 s can be well fitted with a smooth broken power law,

$$F = F_0 \left[\left(\frac{t}{t_\mathrm{b}} \right)^{\omega\alpha_1} + \left(\frac{t}{t_\mathrm{b}} \right)^{\omega\alpha_2} \right]^{-1/\omega}. \quad (1)$$

Our best-fitting parameters are summarized in Table 2. We find that the decay slopes after the two breaks are similar, with a value of $\sim$1.22. The late-time X-ray data at $\sim 4 \times 10^5$ s are also consistent with the predicted behaviour of such a decay slope in the X-ray band.

3.2 Data confronted with the forward shock models

As shown above, the temporal behaviours of the optical and X-ray data are consistent with being achromatic, and the decay slopes after the two breaks observed in the optical light curve are well consistent with the prediction of the forward shock models. The fact that $\alpha_0 = \alpha_x$ is consistent with the forward shock model in the same spectra regime (see also Urata et al. 2007 for a more general discussion of the α_0–α_x relation for the forward shock models). We find no spectral evolution across the two breaks from the X-ray data. The derived β_X are 1.09 ± 0.15 and 1.03 ± 0.10, respectively, for the integrated X-ray spectra at $t < 2200$ s and $t > 2200$ s. Inspecting the spectral index β_X and the temporal decay index α_X in the normal decay segment, one finds good agreement between data and the forward shock model closure relation in the spectral regime $\nu > \max(\nu_m,\ \nu_\mathrm{c})$, i.e. $\alpha = (3\beta_\mathrm{X} - 1)/2 = 1.14 \pm 0.23$, where ν_m and ν_c are the typical and cooling frequencies of synchrotron radiation, respectively. Since both optical and X-ray emissions are consistent with the forward shock origin in the normal decay phase, one can naturally attribute the two shallow decay segments to two epochs of energy injection into the blastwave (e.g. Dai & Lu 1998; Zhang & Mészáros 2001; Zhang et al. 2006; Liang, Zhang & Zhang 2007).

3.3 Constraints on the burst environment

The circumburst environment is critical to understand the nature of a GRB. In the literature, usually two types of medium are discussed, namely, a constant-density medium relevant for interstellar medium (ISM) or a stratified stellar wind with a density profile $n \propto r^{-2}$. For the spectral regime identified for GRB 090426, i.e. $\nu > \max(\nu_m, \nu_\mathrm{c})$, unfortunately the observed flux does not depend on the medium density. Consequently, one cannot distinguish the two types of medium. However, since a wind model would undoubtedly point towards a massive star progenitor, we only focus on the constant-density case. According to the analysis in Section 3.2, ν_c should be below the optical band at very early epochs. This would give an interesting constraint on the medium density.

In the constant-density case, the typical synchrotron emission frequency, the cooling frequency and the peak spectral flux density are (Sari, Piran & Narayan 1998; coefficients taken from Yost et al. 2003; Zhang et al. 2007b)

$$\nu_m = 3.3 \times 10^{12}\ \mathrm{Hz} \left(\frac{p-2}{p-1} \right)^2 (1+z)^{1/2} \epsilon_{B,-2}^{1/2} \epsilon_{e,-1}^{2} E_{K,52}^{1/2} t_\mathrm{d}^{-3/2}, \quad (2)$$

$$\nu_\mathrm{c} = 6.3 \times 10^{15}\ \mathrm{Hz}\ (1+z)^{-1/2} (1+Y)^{-2} \epsilon_{B,-2}^{-3/2} E_{K,52}^{-1/2} n^{-1} t_\mathrm{d}^{-1/2}, \quad (3)$$

$$F_{\nu,\max} = 1.6\ \mathrm{mJy} (1+z) D_{28}^{-2} \epsilon_{B,-2}^{1/2} E_{K,52} n^{1/2}, \quad (4)$$

where D is the luminosity distance in units of 10^{28} cm, f_p is a function of p ($f_p \sim 1$ for $p = 2$, Zhang et al. 2007b) and t_d is the observer's time in unit of days. The convention $Q_n = Q/10^n$ is adopted in CGS units. The inverse Compton scattering parameter is

$$Y = \left[-1 + (1 + 4\eta_1 \eta_2 \epsilon_\mathrm{e}/\epsilon_B)^{1/2} \right]/2, \quad (5)$$

where $\eta_1 = \min[1, (\nu_\mathrm{c}/\nu_m)^{(2-p)/2}] \sim 1$ for $p \sim 2.0$ (Sari & Esin 2001), and $\eta_2 \leq 1$ is a correction factor introduced by the Klein–Nishina effect. We take $\eta_2 = 1$ in our analysis, so that the R-band energy flux reads

$$\begin{aligned} \nu_R F_{\nu_R} &= F_{\nu,\max} \nu_\mathrm{c}^{1/2} \nu_m^{(p-1)/2} \nu_R^{(2-p)/2} \\ &= 2.67 \times 10^{-11} f_p\ \mathrm{erg\ s^{-1}\ cm^{-2}} D_{28}^{-2} (1+z)^{(p+2)/4} \\ &\quad \times (1+Y)^{-1} \epsilon_{B,-2}^{(p-2)/4} \epsilon_{e,-1}^{p-1} E_{K,52}^{(p+2)/4} t_\mathrm{d}^{(2-3p)/4} \nu_R^{(2-p)/2}, \end{aligned} \quad (6)$$

where

$$f_p = \left[7.45 \times 10^{-3} \left(\frac{p-2}{p-1} \right)^2 \right]^{(p-1)/2}. \quad (7)$$

Since $p = 2\beta = 2.18 \pm 0.30$, we have $f_p = 6.04 \times 10^{-3}$. One can then derive E_K using the data at any time t_d (Zhang et al. 2007b):

$$\begin{aligned} E_{K,52} = &\left[\frac{\nu_R F_{\nu_R}}{1.61 \times 10^{-13}\ \mathrm{erg\ s^{-1}\ cm^{-2}}} \right]^{4/(p+2)} \\ &\times D_{28}^{8/(p+2)} (1+z)^{-1} t_\mathrm{d}^{(3p-2)/(p+2)} \\ &\times (1+Y)^{4/(p+2)} \epsilon_{B,-2}^{(2-p)/(p+2)} \\ &\times \epsilon_{e,-1}^{4(1-p)/(p+2)} \nu_R^{2(p-2)/(p+2)}. \end{aligned} \quad (8)$$

The analysis above is valid for $p > 2$. From the X-ray data, we find that p is slightly larger than 2. In order to make a rough estimate, we take $p \sim 2$ to simplify equation (8) as

$$E_K, 52 = \frac{\nu_R F_{\nu_R}}{1.61 \times 10^{-13}\ \mathrm{erg\ s^{-1}\ cm^{-2}}} \frac{t_\mathrm{d}}{1+z} \epsilon_{e,-1}^{-1} (1+Y) D_{L,28}^2. \quad (9)$$

The cooling frequency ν_c is given by

$$\begin{aligned} \nu_\mathrm{c} = &6.3 \times 10^{15}\ \mathrm{Hz} \left(\frac{\nu_R F_{\nu_R}}{1.61 \times 10^{-13}\ \mathrm{erg\ s^{-1}\ cm^{-2}}} \right)^{-1/2} \\ &\times (1+Y)^{-5/2} \epsilon_{B,-2}^{-3/2} \epsilon_{e,-1}^{1/2} n^{-1} t_\mathrm{d}^{-1} D_{28}^{-1}. \end{aligned} \quad (10)$$

At $t \sim 100$ s, one has $\nu_R F_{\nu_R} = 4.42 \times 10^{-12}$ erg cm^{-2} s^{-1}, so that

$$\nu_\mathrm{c} = 1.57 \times 10^{17}\ \mathrm{Hz}\ (1+Y)^{-5/2} \epsilon_{B,-2}^{-3/2} \epsilon_{e,-1}^{1/2} n^{-1}. \quad (11)$$

The requirement of $\nu_R > \nu_\mathrm{c}$ at $t \sim 100$ s then gives

$$n > 354 s(\epsilon_e, \epsilon_B), \quad (12)$$

where $s(\epsilon_e, \epsilon_B) = \epsilon_{B,-2}^{-3/2} \epsilon_{e,-1}^{1/2} (1+Y)^{-5/2}$. This already points towards a large medium density. Noting that s would decrease when

ϵ_B increases, we consider an extreme case of energy equipartition among radiating electrons, magnetic field and baryons, i.e. $\epsilon_e = 1/3$, $\epsilon_B = 1/3$. In this case, we still get $n > 11.2\,\mathrm{cm}^{-3}$. Such a dense medium is inconsistent with the naive expectation of a compact star merger progenitor, which tends to occur in low-density medium as the compact binary escapes from the star-forming region due to the natal kicks during the births of the two neutron stars. The high density, on the other hand, is consistent with that expected for a massive star that was born in a high-density star-forming region such as a molecular cloud (e.g. Chevalier, Li & Fransson 2004).

Recall that a stellar wind medium also suggests a massive star connection, we therefore conclude that the high ISM density would favour a burst born in a region of ongoing star formation, and hence favour a massive star progenitor (or a Type II GRB) for GRB 090426.

4 DISCUSSION AND CONCLUSIONS

We have presented the early optical afterglow observations of GRB 090426 with TNT and LOAO. Our well-sampled optical afterglow light curve from ∼90 to 10^4 s after the GRB trigger seems to exhibit two energy-injection phases that ended at ∼230 and 7100 s, respectively. The temporal behaviour of the observed X-rays is consistent with the optical emission. We show that both the optical and X-ray afterglows are consistent with the forward shock model in the spectral regime $\nu > \max(\nu_m,\ \nu_c)$. Although the medium type (ISM versus wind) cannot be distinguished, we can make a case of the massive star (Type II) origin of the GRB. For a constant-density medium, the required medium density is found to be very high (equation 12), inconsistent with the expectation of a compact star merger (Type I) progenitor. A massive star progenitor forming in a high-density star-forming region (e.g. molecular cloud) is consistent with the data. If the circumburst medium is a stellar wind, then it also directly points towards a massive star progenitor. We therefore conclude that the afterglow data of the short GRB 09046 strongly suggest that it is a Type II GRB.

GRB 090426 is of great interest because of its short duration ($T_{90} \sim 0.33$ s in the burst frame) and high redshift ($z = 2.609$). Its redshift significantly exceeds the previous spectroscopically confirmed high redshifts of short GRBs, e.g. GRB 070714B ($z = 0.904$; Graham et al. 2009), GRB 051121A ($z = 0.546$; Soderberg et al. 2006b), GRB 070429 ($z = 0.902$; Cenko et al. 2008) and GRB 090510 ($z = 0.903$; Rau, McBreen & Kruehler 2009). Its host galaxy is a blue, luminous and star-forming galaxy (Levesque et al. 2010a), similar to the host galaxies of typical Type II GRBs (Levesque et al. 2010b). The spectral energy correlation is also consistent with being a Type II GRB. Here we present a third argument in favour of its Type II origin, based on early afterglow observation and modelling. It is interesting to note that with the new classification method proposed by Lv et al. (2010), GRB 090426 is well grouped into Type II GRBs, in contrast to other short GRBs such as GRB 051221 and GRB 070714B. We also noted that GRB 090426 shares some similar properties with two other Type II bursts, GRB 040924 and GRB 050416A. The first was a short-duration (1.2–1.5 s), soft-spectrum (Huang et al. 2005) and a SN 1998bw-like supernova-associated burst (Soderberg et al. 2006a; Wiersema et al. 2008). The second burst also exhibited a soft spectrum and a short duration in the rest frame ($T_{90} = 2.4$ s, $z = 0.6528$), which is associated with a SN 1998bw-like supernova (Soderberg et al. 2007), and is located in a circumburst medium with a large density variation.

Finally, GRB 090426 has reinforced the conclusion that burst duration alone cannot be used to judge the physical nature of a GRB, as discussed by Donaghy et al. (2006), Zhang et al. (2007a),[4] Levan et al. (2007)[5] and Zhang et al. (2009).[6] Multiwavelength observational campaigns are essential to unveil the physical nature of GRBs.

ACKNOWLEDGMENTS

The authors thank the anonymous referee for helpful suggestions and comments, and Massimiliano De Pasquale for correcting an error in the early version. This work made use of data supplied by the UK *Swift* Science Data Centre at the University of Leicester. It is partially supported by the National Natural Science Foundation of China under grants Nos 10673014, 10803008 and 10873002 and the National Basic Research Programme ('973' Programme) of China under Grant 2009CB824800. It is also partly supported by grants NSC 98-2112-M-008-003-MY3 (YU) and by NASA NNX09AT66G, NNX10AD48G and NSF AST-0908362 (BZ). E-WL also acknowledges the support from the Guangxi SHI-BAI-QIAN project (Grant 2007201), the Guangxi Science Foundation (2010GXNSFC013011)the programme for 100 Young and Middle-aged Disciplinary Leaders in Guangxi Higher Education Institutions and the research foundation of Guangxi University (M30520). MI and YS are supported by the Korea Science and Engineering Foundation (KOSEF) grant No. 2009-0063616, funded by the Korean government (MEST). K-YH was supported by NSC-99-2112-M-001-002-MY3.

REFERENCES

Adelman-McCarthy J. K. et al., 2008, ApJS, 175, 297
Antonelli L. A. et al., 2009, A&A, 507, L45
Barthelmy S. D. et al., 2005, Nat, 438, 994
Belczynski K., Holz D. E., Fryer C. L., Berger E., Hartmann D. H., O'Shea B., 2010, ApJ, 708, 117
Berger E. et al., 2005, ApJ, 634, 501
Berger E. et al., 2007, ApJ, 664, 1000
Campana S. et al., 2006, Nat, 442, 1008
Cenko S. B. et al., 2008, preprint (arXiv:0802.0874)
Chevalier R. A., Li Z.-Y., Fransson C., 2004, ApJ, 606, 369
Cummings J. R. et al., 2009, GRB Coordinates Network, 9254, 1
Dai Z. G., Lu T., 1998, A&A, 333, L87
Donaghy T. Q. et al., 2006, preprint (astro-ph/0605570)
Eichler D., Livio M., Piran T., Schramm D. N., 1989, Nat, 340, 126
Evans P. A. et al., 2009, MNRAS, 397, 1177
Fong W., Berger E., Fox D. B., 2010, ApJ, 708, 9
Fox D. B. et al., 2005, Nat, 437, 845
Fynbo J. P. U. et al., 2006, Nat, 444, 1047
Galama T. J. et al., 1998, Nat, 395, 670
Gal-Yam A. et al., 2006, Nat, 444, 1053
Gehrels N. et al., 2005, Nat, 437, 851
Gehrels N. et al., 2006, Nat, 444, 1044
Graham J. F. et al., 2009, ApJ, 698, 1620
Greiner J. et al., 2009, ApJ, 693, 1610
Han W. et al., 2005, PASJ, 57, 821
Hjorth J. et al., 2003, Nat, 423, 847

[4] Both teams proposed that some long GRBs can be physically associated with compact star mergers, but did not discuss that short bursts can be physically related to massive star core collapses.
[5] These authors pointed out that some long GRBs are rest-frame short bursts.
[6] These authors first mentioned the possibility that some observer-frame short bursts can originate from massive stars.

Huang K. Y. et al., 2005, ApJ, 628, L93
Im M., Jeon Y., Lee I., Jeon Y.-B., Urata Y., 2009, GRB Coordinates Network, 9276, 1
Kann D. A. et al., 2007, preprint (arXiv:0712.2186)
Kann D. A. et al., 2008, preprint (arXiv:0804.1959)
Kouveliotou C., Meegan C. A., Fishman G. J., Bhat N. P., Briggs M. S., Koshut T. M., Paciesas W. S., Pendleton G. N., 1993, ApJ, 413, L101
Lee I., Im M., Urata Y., 2010, J. Korean Astron. Soc., 43, 95
Levan A. J. et al., 2006, ApJ, 648, L9
Levan A. J. et al., 2007, MNRAS, 378, 1439
Levesque E., Chornock R., Kewley L., Bloom J. S., Prochaska J. X., Perley D. A., Cenko S. B., Modjaz M., 2009, GRB Coordinates Network, 9264, 1
Levesque E. M. et al., 2010a, MNRAS, 401, 963
Levesque E. M., Berger E., Kewley L. J., Bagley M. M., 2010b, AJ, 139, 694
Liang E.-W., Zhang B.-B., Zhang B., 2007, ApJ, 670, 565
Lin L., Liang E.-W., Zhang B.-B., Zhang S. N., 2008, in AIP Conf. Proc. Vol. 1065, Nanjing gamma-ray burst conference. Am. Inst. Phys., New York, p. 39
Lin L., Liang E. W., Zhang B. B., Zhang S. N., 2010, preprint (arXiv:0906.3057)
Lv H., Liang E., Zhang B., Zhang B., 2010, preprint (arXiv:1001.0598)
McGlynn S., Foley S., McBreen S., Hanlon L., O'Connor R., Carrillo A. M., McBreen B., 2008, A&A, 486, 405
Narayan R., Paczyński B., Piran T., 1992, ApJ, 395, L83
Norris J. P., Bonnell J. T., 2006, ApJ, 643, 266
Paczyński B., 1998, ApJ, 494, L45
Perley D. A. et al., 2009, ApJ, 696, 1871
Piran T., 2004, Rev. Modern Phys., 76, 1143
Rau A., McBreen S., Kruehler T., 2009, GRB Coordinates Network, 9353, 1
Rumyantsev V., Antoniuk K., Pozanenko A., 2009, GRB Coordinates Network, 9320, 1
Sakamoto T. et al., 2009, ApJ, 693, 922
Salvaterra R. et al., 2009, Nat, 461, 1258
Sari R., Esin A. A., 2001, ApJ, 548, 787
Sari R., Piran T., Narayan R., 1998, ApJ, 497, L17
Sato G. et al., 2009, GRB Coordinates Network, 9263, 1
Schlegel D. J., Finkbeiner D. P., Davis M., 1998, ApJ, 500, 525
Soderberg A. M. et al., 2004, Nat, 430, 648
Soderberg A. M. et al., 2006a, ApJ, 636, 391
Soderberg A. M. et al., 2006b, ApJ, 650, 261
Soderberg A. M. et al., 2007, ApJ, 661, 982
Tanvir N. R. et al., 2009, Nat, 461, 1254
Thoene C. C. et al., 2009, GRB Coordinates Network, 9269, 1
Urata Y. et al., 2003, ApJ, 595, L21
Urata Y. et al., 2005, Nuovo Cimento C, 28, 775
Urata Y. et al., 2007, ApJ, 668, L95
Villasenor J. S. et al., 2005, Nat, 437, 855
Virgili F. J., Zhang B., O'Brien P., Troja E., 2009, preprint (arXiv:0909.1850)
Wiersema K. et al., 2008, A&A, 481, 319
Woosley S. E., 1993, ApJ, 405, 273
Woosley S. E., Bloom J. S., 2006, ARA&A, 44, 507
Xin L. P., Zheng W. K., Qiu Y. L., Wei J. Y., Wang J., Deng J. S., Urata Y., Hu J. Y., 2009, GRB Coordinates Network, 9255, 1
Xin L. P. et al., 2010, MNRAS, 401, 2005
Yost S. A., Harrison F. A., Sari R., Frail D. A., 2003, ApJ, 597, 459
Zhang B., Mészáros P., 2001, ApJ, 552, L35
Zhang B., Mészáros P., 2004, Int. J. Modern Phys. A, 19, 2385
Zhang B., Fan Y. Z., Dyks J., Kobayashi S., Mészáros P., Burrows D. N., Nousek J. A., Gehrels N., 2006, ApJ, 642, 354
Zhang B., Zhang B.-B., Liang E.-W., Gehrels N., Burrows D. N., Mészáros P., 2007a, ApJ, 655, L25
Zhang B. et al., 2007b, ApJ, 655, 989
Zhang B. et al., 2009, ApJ, 703, 1696
Zheng W.-K. et al., 2008, Chinese J. Astron. Astrophys., 8, 693

This paper has been typeset from a TEX/LATEX file prepared by the author.